Molecular Crystals and Liquid Crystals Incorporating Nonlinear Optics

Publication details, including instructions for authors and subscription information:
http://www.tandfonline.com/loi/gmcl17

Crosstalk In Multiplexed Liquid-Crystal Matrix Displays Due to Electrode Resistance

J. Nehring [a] & T. J. Scheffer [b]

[a] Asea Brown Boveri Corporate Research, CH-5405, Baden-Dättwil, Switzerland

[b] Tektronix Laboratories, Beaverton, OR, 97077, USA

Version of record first published: 22 Sep 2006.

To cite this article: J. Nehring & T. J. Scheffer (1990): Crosstalk In Multiplexed Liquid-Crystal Matrix Displays Due to Electrode Resistance, Molecular Crystals and Liquid Crystals Incorporating Nonlinear Optics, 191:1, 87-95

To link to this article: http://dx.doi.org/10.1080/00268949008038582

Mol. Cryst. Liq. Cryst. 1990, Vol. 191, pp. 87–95
Reprints available directly from the publisher
Photocopying permitted by license only

Printed in the United States of America

Crosstalk in Multiplexed Liquid-Crystal Matrix Displays Due to Electrode Resistance

J. NEHRING and T. J. SCHEFFER†

Asea Brown Boveri Corporate Research, CH-5405 Baden-Dättwil, Switzerland and †Tektronix Laboratories, Beaverton, OR 97077, USA

(*Received October 2, 1989*)

1. INTRODUCTION

A new type of liquid crystal matrix display has recently become known under the name "supertwist display" due to its 2–3 times higher twist angle of the liquid crystal structure compared to the standard 90° twisted nematic display. These displays make use of an electro-optic effect which combines a steep voltage vs. contrast characteristic with high contrast and brightness values.[1] Multiplexing of more than 200 lines has become possible allowing applications in laptop computers and word processing systems where more than 10^5 picture elements ("pixels") per display are required. The upper limit of multiplexable lines has not been determined and depends on many factors including the material properties of the liquid crystal, the cell technology and uniformity of the liquid crystal layer. An important factor is the finite electrode conductivity which has only received brief attention in the literature.[2–4] In this paper we investigate in more detail the influence that the finite electrical conductivity of the display electrodes has on the multiplexing limit.

Consider a liquid crystal layer with electrodes arranged as a set of M parallel stripes of width b (in y direction) on the one substrate, the row electrodes, and another set of N parallel stripes of width b' (in x direction) on the other substrate, the column electrodes (Figure 1). In present computer displays typical values are M = 200 or 240 and N = 640.[5] Let the electrical surface resistivity (measured in Ohms per square) be ρ for the first set of stripes and ρ' for the second set. The total resistance of a stripe in y or x direction, respectively, is then given by

$$R_{tot} = \rho\, N\, b'/b \tag{1}$$

$$R'_{tot} = \rho'\, M\, b/b' . \tag{2}$$

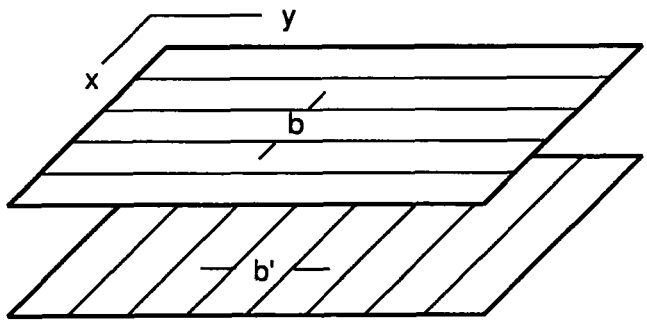

FIGURE 1 Row and column electrodes in a liquid crystal matrix display.

The area of overlap of the k-th stripe of the first set with the l-th stripe of the second set defines the pixel (k,l). The pixel dimensions b and b' are typically on the order of 0.5 mm. The surface resistivity of indium-tin-oxide ('ITO') electrode layers falls into the range of $10^1 - 10^3\Omega/\square$. Thus, the pixel resistances in y and x direction

$$R = \rho\, b'/b \tag{3}$$

$$R' = \rho'\, b/b' \tag{4}$$

are of the order $10^1 - 10^3\ \Omega$. Because of the dielectric anisotropy of the liquid crystal the electrical capacitance C_{kl} of the pixel (k,l) depends on the voltage across the pixel. For simplicity we will assume that at most only two values (C_{on} or C_{off}) may occur, depending on whether the pixel is in the "on" or "off" state. In addition, the dielectric anisotropy will be assumed to be frequency independent. If we define

$$\overline{C} = (C_{on} + C_{off})/2 \tag{5}$$

$$\gamma = (C_{on} - C_{off})/C_{off}\ , \tag{6}$$

we may write for the pixel capacitance

$$C_{kl} = \overline{C}\left(1 + \frac{\gamma}{\gamma + 2}\,\eta_{kl}\right) \tag{7}$$

where

$$\eta_{kl} = \begin{cases} +1\ ;\ \text{pixel "on"} \\ -1\ ;\ \text{pixel "off"} \end{cases} \tag{8}$$

Assuming a mean dielectric constant of 10, a spacing between the substrates of $d = 7\ \mu$m and $b = b' = 0.5$ mm, a value of $\overline{C} \approx 3$ pF is found for the mean pixel capacitance. γ is typically on the order of 1.

We distinguish two sets of electrical driving signals.[6] There are M "strobe" signals $F_k(t)$, $(k = 1, \ldots, M)$ which are applied to the row electrodes and N "data" signals $G_l(t)$, $(l = 1, \ldots, N)$ which are applied to the column electrodes. All signals are periodic in time t with a common period T. In addition, we assume

$$F_k(t + T/2) = -F_k(t) \tag{9}$$

$$G_l(t + T/2) = -G_l(t) \quad . \tag{10}$$

The period is typically $T \approx 30$ ms which prevents flicker to appear to the human eye and the half-period sign reversal ensures that no detrimental electrochemical effects occur in the display. We may define strobe and data signals in the time interval $0 \leq t < T/2$ as

$$F_k(t) = \begin{cases} P\ ; & (k-1)\tau \leq t < k\tau \\ 0\ ; & \text{otherwise} \end{cases} \tag{11}$$

$$G_l(t) = -\eta_{kl} P/\sqrt{M}\ ; \quad (k-1)\tau \leq t < k\tau \tag{12}$$

where $\tau = T/(2M)$ is the width of a strobe pulse and P is its height (in volts). In Figure 2 strobe and data signals as defined by Equations (11) and (12) are shown

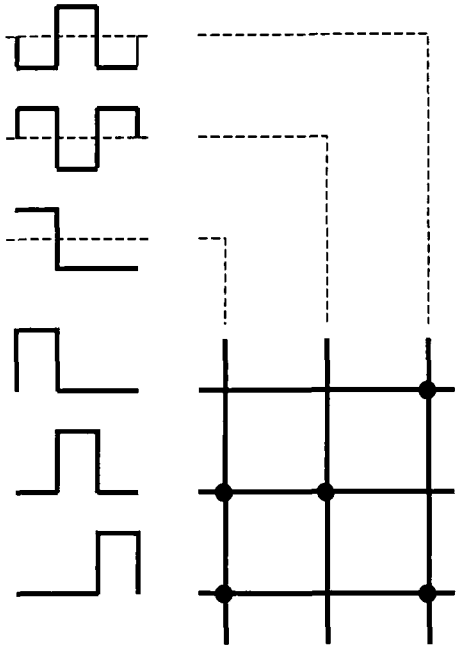

FIGURE 2 Strobe and data signals.

schematically with the black dots in the matrix symbolizing "on" pixels. (In actual displays slight modifications of the strobe and data signals are used so that all driving signals will be of the same polarity. This modification has practically no influence on the crosstalk effects to be studied.)

For ideal electrodes ($R = R' = 0$), the effective voltage, i.e. the root-mean-square (rms) voltage, experienced by the pixel (k,l) is given by

$$\bar{V}_{kl} = \frac{\sqrt{2}P}{\sqrt{M}} \sqrt{1 + \frac{\eta_{kl}}{\sqrt{M}}} \quad . \tag{13}$$

According to this equation, there are two rms voltages present in the matrix: an "on" voltage when $\eta_{kl} = 1$ and an "off" voltage when $\eta_{kl} = -1$. Equation (13), however, is no longer valid when R and R' are different from zero. A voltage distribution will then exist such that different voltages are seen by different "on" pixels and by different "off" pixels, respectively. Some "on" pixels may even experience lower voltages than "off" pixels. In the following these effects will be studied.

2. DISCRETE ELEMENT MODEL

In order to compute the voltage distribution in a multiplexed liquid crystal matrix display, we describe each row electrode of Figure 1 by a series of N resistors of size R and each column electrode by a series of M resistors of size R'. R and R' are given by Equations (3) and (4). Rows and columns are connected by the liquid crystal capacitors C_{kl} as shown in Figure 3. The finite ohmic resistivity of the liquid crystal will not be taken into account.

We expand the driving signals (11) and (12) into Fourier series

$$F_k(t) = \sum_{\mu=-\infty}^{\infty} A_{k,\mu}\, e^{i\mu\omega_0 t} \tag{14}$$

$$G_l(t) = \sum_{\mu=-\infty}^{\infty} B_{l,\mu}\, e^{i\mu\omega_0 t} \tag{15}$$

where $\omega_o = 2\pi/T$. The Fourier coefficients $A_{k,\mu}$ and $B_{l,\mu}$ are different from zero only for odd values of μ. In addition, $A_{k,\mu} = (A_{k,-\mu})^*$ and $B_{l,\mu} = (B_{lk,-\mu})^*$ with the asterisk indicating the complex conjugate. For the purpose of computing rms

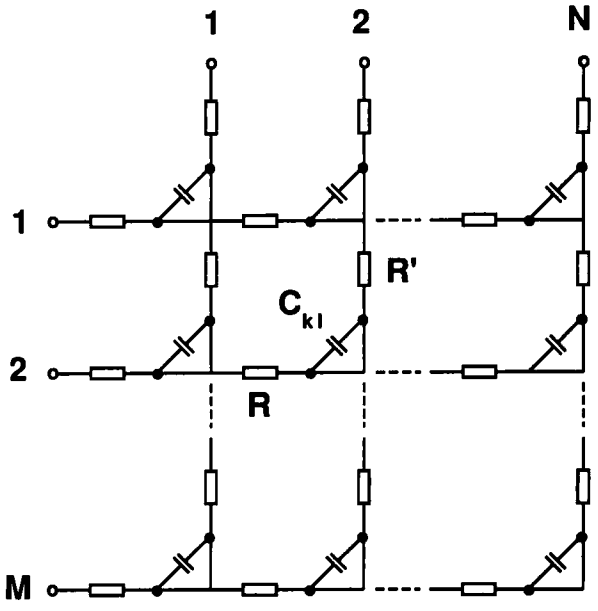

FIGURE 3 Schematic of the discrete element model of a liquid crystal matrix display.

voltages, we may thus replace the system (14)–(15) by the equivalent system

$$U_{ko}(t) = \sum_{\lambda=1}^{\infty} u_{ko,\lambda}\, e^{i(2\lambda-1)\omega_0 t} \tag{16}$$

$$V_{ol}(t) = \sum_{\lambda=1}^{\infty} v_{ol,\lambda}\, e^{i(2\lambda-1)\omega_0 t} \tag{17}$$

where

$$u_{ko,\lambda} = \frac{2\sqrt{2}P}{(2\lambda-1)\pi} \sin\frac{(2\lambda-1)\pi}{2M}\, e^{-i(2\lambda-1)\pi k/M} \tag{18}$$

$$v_{ol,\lambda} = \frac{2\sqrt{2}P}{(2\lambda-1)\pi} \sin\frac{(2\lambda-1)\pi}{2M} \frac{1}{\sqrt{M}} \sum_{\sigma=1}^{M} \eta_{\sigma l}\, e^{-i(2\lambda-1)\pi\sigma/M} \tag{19}$$

We denote the electric potentials on the two sides of a pixel capacitor C_{kl} by U_{kl}

(strobe side) and V_{kl} (data side). Both potentials may be expanded into series corresponding to those of Equations (16) and (17) with the Fourier coefficients denoted by $u_{kl,\lambda}$ and $v_{kl,\lambda}$, respectively. Considering the current flow in the network of Figure 3, it is easy to deduce that the following relations hold between the Fourier coefficients of a given index λ:

$$(u_{k(l-1),\lambda} - u_{kl,\lambda})/R = i(2\lambda-1)\omega_0 \sum_{\sigma=1}^{N} C_{k\sigma}(u_{k\sigma,\lambda} - v_{k\sigma,\lambda}) \tag{20}$$

$$(v_{kl,\lambda} - v_{(k-1)l,\lambda})/R' = i(2\lambda-1)\omega_0 \sum_{\mu=k}^{M} C_{\mu l}(u_{\mu l,\lambda} - v_{\mu l,\lambda}) \; . \tag{21}$$

Here i is the imaginary unit. It is the meaning of Equation (20) that the current flowing through the l-th resistor (counted from the left in Figure 3) of the k-th row is equal to the sum of currents through the capacitors C_{kl}, $C_{k(l+1)}$, . . . , C_{kN}. Correspondingly, Equation (21) refers to the current through the k-th resistor in the l-th column. Using Equation (7) and subtracting two Equations (20) which differ by 1 in the index l and two Equations (21) which differ by 1 in the index k leads to the following recursion formulas for the determination of $u_{kl,\lambda}$ and $v_{kl,\lambda}$:

$$u_{k(l+1),\lambda} - 2u_{kl,\lambda} + u_{k(l-1),\lambda} = i(2\lambda-1)\,\Gamma\,(1+\frac{\gamma}{\gamma+2}\eta_{kl})\,(u_{kl,\lambda} - v_{kl,\lambda}) \tag{22}$$

$$v_{(k+1)l,\lambda} - 2v_{kl,\lambda} + v_{(k-1)l,\lambda} = -i(2\lambda-1)\,\Gamma'\,(1+\frac{\gamma}{\gamma+2}\eta_{kl})\,(u_{kl,\lambda} - v_{kl,\lambda}) \tag{23}$$

where Γ and Γ' are dimensionless parameters defined by

$$\Gamma = \omega_0 R\overline{C} \; , \qquad \Gamma' = \omega_0 R'\overline{C} \; . \tag{24}$$

The boundary conditions are given by Equations (18) and (19) and by the following Equations (25):

$$u_{k(N+1),\lambda} = u_{kN,\lambda} \; , \qquad v_{(M+1)l,\lambda} = v_{Ml,\lambda} \tag{25}$$

The rms voltage effective at the pixel (k,l) is obtained from

$$\bar{V}_{kl} = \sqrt{\sum_{\lambda=1}^{\infty} |u_{kl,\lambda} - v_{kl,\lambda}|^2} \tag{26}$$

We notice from Equations (18)–(19) and (22)–(26) that the voltage distribution in a multiplexed M × N matrix is governed by the information pattern η_{kl}, the anisotropy γ of the "on"/"off" capacitances, and the parameters Γ and Γ'.

3. RESULTS

We have solved Equations (22)–(23) numerically for various matrix sizes and information patterns assuming different values for Γ, Γ' and γ. A typical result is shown in Figure 4 for a 45 × 45 matrix displaying the letters of the alphabet. $\Gamma = \Gamma' = 10^{-5}$ and $\gamma = 1.0$ has been assumed for the computation. In Figure 4 the voltage distribution has been made visible using a six step greyscale with brighter pixels corresponding to higher voltages. The most pronounced feature, which may also be found in actual displays, is the strong voltage drop in columns with a frequent change of "on" and "off" states.[2] Such columns are addressed by higher frequency data signals than columns with fewer changes of "on" and "off" pixels, and higher frequencies are attenuated more strongly. For the Γ value chosen, some "on" pixels close to the lower edge of the matrix experience voltages nearly as low as an "off" pixel. For square pixels with $\overline{C} \approx 3$ pF and $\omega_o \approx 200$ Hz, the value $\Gamma = 10^{-5}$ corresponds to a surface resistivity of 17 $k\Omega/\square$.

In order to find a general rule on how small the electrode resistivity has to be if no sizable voltage drop is to occur in a matrix of a given size, we have investigated the unfavorable case (frequent "on"/"off" changes) of the micro-checkerboard pattern

$$\eta_{kl} = (-1)^{k+l} \tag{27}$$

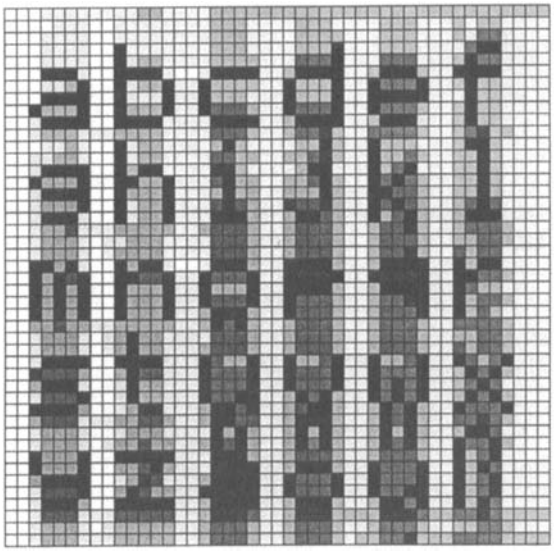

FIGURE 4 Computed voltage distribution in a 45 × 45 matrix ($\Gamma = \Gamma' = 10^{-5}$, $\gamma = 1$). Increasing voltage is indicated by brighter pixels.

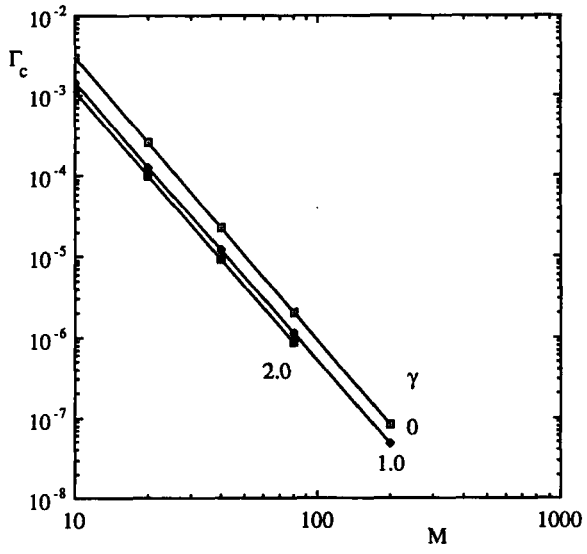

FIGURE 5 Critical values Γ_c (see text) for square matrices as function of matrix dimension M ($\Gamma = \Gamma'$, $\gamma = 0, 1, 2$).

having an "on" pixel in the upper left corner. Assuming again $\Gamma = \Gamma'$, we have determined the critical value Γ_c for which the highest "off" voltage occurring in the matrix is equal to the lowest "on" voltage. An upper limit for the electrode resistivity is then obtained from the condition $\Gamma = \Gamma' << \Gamma_c$. The result of the computation obtained for square matrices of up to 200 × 200 pixels is shown in Figure 5 for γ values of 0, 1.0 and 2.0. Evaluation of the linear relationship between $\log(\Gamma_c)$ and $\log(M)$ leads to

$$\Gamma_c = w\, M^{-z} \tag{28}$$

with $z \approx 3.5$ and $w \approx 9.3$, 3.8 and 3.0 for the three γ values 0, 1.0 and 2.0. It thus follows the rule that an increase of the matrix size from M × M to (2M) × (2M) increases Γ_c by a factor of about 10. Also, higher values of γ entail lower values of Γ_c. For a simple one-dimensional RC network one would expect an exponent $z = 3$, taking into account that the data frequency of the micro-checkerboard increases proportional to M. The higher exponent reported here is a consequence of the more complicated network.

Considering the case M = N = 200 with $\gamma = 1.0$, we obtain from Equation (28) that $\Gamma_c = 3.4 \times 10^{-8}$. Using again a typical frame frequency of $\omega_o \approx 200$ Hz and $\overline{C} \approx 3$ pF we deduce that the electrode resistivity should be well below 50 Ω/□. For M = N = 400 the corresponding value would be 5 Ω/□. Since ITO layers with surface resistivities as low as 1 Ω/□ having adequate optical transmission are not readily available, it can be concluded that 400 line displays will require some augmentation of the electrode conductivity, perhaps through the addition of fine-line metallization to the electrodes.

In addition to square matrices we have also studied crosstalk effects in rectangular matrices. Considering again a micro-checkerboard pattern, it was found that Γ_c decreases by a factor of about 10 when the matrix size increases from M × M to M × (4M). Practically this effect could be reduced by driving the matrix rows from both sides either with a dual set of drivers or a wrap-around sheet of flex connector.

4. CONCLUDING REMARKS

The results reported in the preceding chapter are based on the model shown in Figure 3. While the description of the electrodes by discrete resistors is a good approximation, in a refined model the description of the voltage dependence of the pixel capacitors would have to be improved. A complete study of crosstalk effects also requires the inclusion of the frequency dependence of the dielectric anisotropy[7] and the output impedances of the driver circuits.

References

1. T. J. Scheffer and J. Nehring, *Appl. Phys. Lett.*, **45**, 1021 (1984).
2. J. Duchene, *Displays*, **7**, 3 (1986).
3. H. Kawakami, H. Hanmura and E. Kaneko, Society for Information Display (SID) Digest of Technical Papers, **10**, 28 (1980); H. Hanmura, H. Kawakami and E. Kaneko, *Displays*, **2**, 178 (1981).
4. F. Tacheuchi, A. Okazaki, K. Kawasaki and H. Yamada, *Mol. Cryst. Liq. Cryst.*, **66**, 83 (1981). H. Ideno, K. Horikiri and H. Arai, Japan Display '83, The 3rd International Display Research Conference, post-deadline paper PD5.
5. Commercial dot matrix displays generally consist of two half-matrices of the size given, leading to pixel arrays of 400 × 640 and 480 × 640. Since the two half-matrices do not share the same column electrodes, M and N defined here refer to the dimension of a half-matrix.
6. P. M. Alt and P. Pleshko, *IEEE Trans. Electron Devices*, **ED-21**, 146 (1974).
7. J. R. Hughes, *IEE Proc.*, **133 Pt. 1**, 145 (1986).